Virologica Sinica 38 (2023) 827–831

Contents lists available at ScienceDirect

Virologica Sinica

journal homepage: www.keaipublishing.com/en/journals/virologica-sinica
www.virosin.org

Letter

Comparative study of the pathogenicity of the mosquito origin strain and duck origin strain of Tembusu virus in ducklings and three-week-old mice

Xiaoli Wang [a,1], Yu He [a,1], Jiaqi Guo [a,1], Zhen Wu [a], Andres Merits [d], Mingshu Wang [a,b,c], Renyong Jia [a,b,c], Dekang Zhu [b,c], Mafeng Liu [a,b,c], Xinxin Zhao [a,b,c], Qiao Yang [a,b,c], Ying Wu [a,b,c], Shaqiu Zhang [a,b,c], Juan Huang [a,b,c], Xumin Ou [a,b,c], Qun Gao [a,b,c], Di Sun [a,b,c], Anchun Cheng [a,b,c,*], Shun Chen [a,b,c,*]

[a] Institute of Preventive Veterinary Medicine, Sichuan Agricultural University, Chengdu, 611130, China
[b] Research Center of Avian Disease, College of Veterinary Medicine, Sichuan Agricultural University, Chengdu, 611130, China
[c] Key Laboratory of Animal Disease and Human Health of Sichuan Province, Sichuan Agricultural University, Chengdu, 611130, China
[d] Institute of Technology, University of Tartu, Tartu, 999148, Estonia

Dear Editor,

Duck Tembusu virus (DTMUV) is the causative agent of a new, acute and severe infectious disease in ducks (Su et al., 2011). TMUV was first isolated from *Culex tritaeniorhynchus* in Malaysia in 1955 (Platt et al., 1975), and this strain is regarded as a reference strain. In our previous study, an infectious clone for the mosquito-derived Tembusu virus prototypical strain MM_1775 (GenBank: JX477685.2) was constructed, and the rMM_1775 virus was rescued successfully (Wang et al., 2021). And the TMUV strain rCQW1 was rescued by a reverse genetic system using the viral RNAs of CQW1 (GenBank: KM233707.1) (Chen et al., 2018; Guo et al., 2020), which was isolated from ducks in 2013 (Zhu et al., 2015).

Here, we compared the pathogenicity of mosquito (rMM_1775) and duck TMUV (rCQW1) strains in ducks and mice. First, to explore the difference in pathogenicity of TMUV in mice, three-week-old Kunming mice were infected with rMM_1775 and rCQW1 at a dose of $10^{4.5}$ $TCID_{50}$ by intraperitoneal injection (i.p.) or intracranial injection (i.c.), and the clinical signs and body weight were observed and recorded for 14 days (Fig. 1A). In the i.c. group, mice exhibited significant clinical symptoms after inoculation with the rMM_1775 virus, including depression, anorexia, hind limb paralysis, yellow mucus in the eyes and inability to open eyes at 6 days post-infection (dpi) (Fig. 1B). The body weight of the rMM_1775 i.c. group started to sharply decrease from 4 dpi compared with that of the mock group, and eight mice died throughout the experiment (Fig. 1C). In the rMM_1775 i.p., rCQW1 i.c. and rCQW1 i.p. groups, mice did not show any clinical signs, and the body weight showed no changes compared with that of the mock group (Fig. 1C and D). In addition, the viral loads in tissues were detected at 2, 5 and 8 dpi. However, the virus could be detected only in the brains of the duck TMUV- and mosquito TMUV-infected mice, which peaked at 5 dpi (Fig. 1E). These results indicated that three-week-old mice could be infected with TMUV by intracranial injection and that the mosquito strain rMM_1775 was more pathogenic to mice than the duck strain rCQW1.

Then, to explore the difference in pathogenicity of TMUV in specific-pathogen-free (SPF) ducklings, 5-day-old SPF ducklings were infected with rMM_1775 or rCQW1 at a dose of 10^5 $TCID_{50}$ by intramuscular injection (i.m.), and the clinical signs and body weight were observed and recorded for 14 days (Fig. 1F). The group injected with the rCQW1 virus through the i.m. route showed obvious clinical symptoms, including depression, anorexia, and paralysis of the lower limbs (Supplementary Fig. S1). Three ducklings died throughout the experiment (Fig. 1G); two died at 5 dpi, and one died at 6 dpi. Compared with that of the mock group, the body weight gain of the rCQW1 group was significantly lower (Fig. 1H). The rMM_1775-infected ducklings did not show any clinical changes or body weight difference from the mocks during the 14 days. The viral titers obtained from the different tissues of the TMUV-inoculated ducks that were euthanized at 3, 5 and 7 dpi are shown in Fig. 1I–K. Virus could be detected in the brains of the ducklings when administered through the i.m. route, indicating that rCQW1 could pass through the blood-brain barrier (Fig. 1I). As shown, virus was detected in all tested tissues (heart, liver, spleen, lung, kidney and thymus) at 3 dpi, indicating rapid systemic dissemination of rCQW1. Viral loads in all examined tissues reached maximum levels at 3 dpi and gradually decreased, and the virus was mostly cleared from 5 to 7 dpi. rMM_1775 was not detectable in the heart and liver at 5 dpi or in any tissue except the spleen at 7 dpi. The viral titers in the heart from the ducklings

* Corresponding authors.
E-mail addresses: chenganchun@vip.163.com (A. Cheng), shunchen@sicau.edu.cn (S. Chen).
[1] Xiaoli Wang, Yu He, and Jiaqi Guo contributed equally to this work.

https://doi.org/10.1016/j.virs.2023.07.006

Available online 5 August 2023

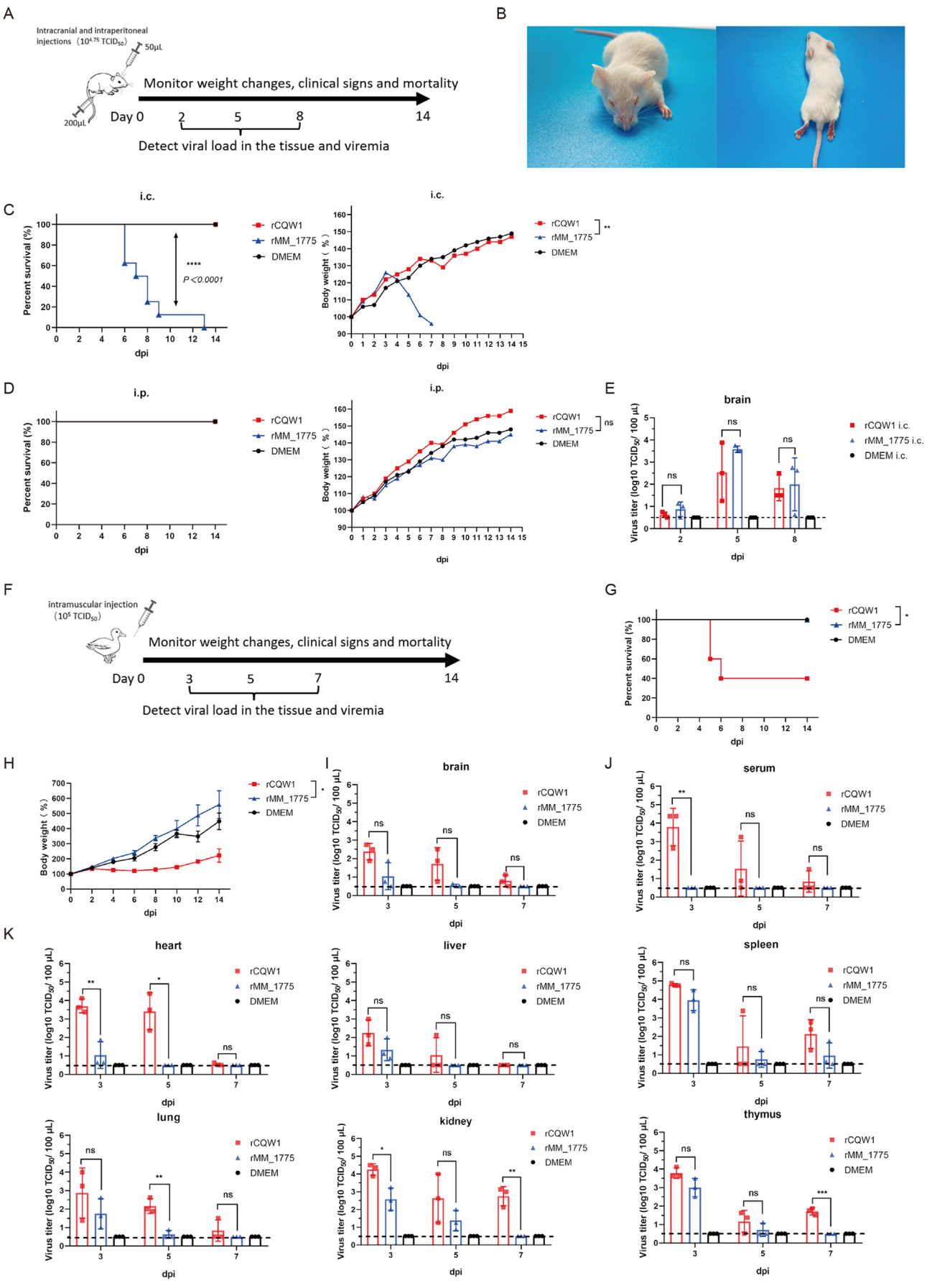
A
Intracranial and intraperitoneal injections (10^4.75 TCID50)
50μL
200μL
Monitor weight changes, clinical signs and mortality
Day 0
2
5
8
14
Detect viral load in the tissue and viremia
B
C
i.c.
Percent survival (%)
dpi
****
P <0.0001
rCQW1
rMM_1775
DMEM
Body weight (%)
**
D
i.p.
ns
E
brain
Virus titer (log10 TCID50/ 100 μL)
rCQW1 i.c.
rMM_1775 i.c.
DMEM i.c.
F
intramuscular injection
(10^5 TCID50)
3
5
7
G
*
H
I
J
serum
K
heart
liver
spleen
lung
kidney
thymus

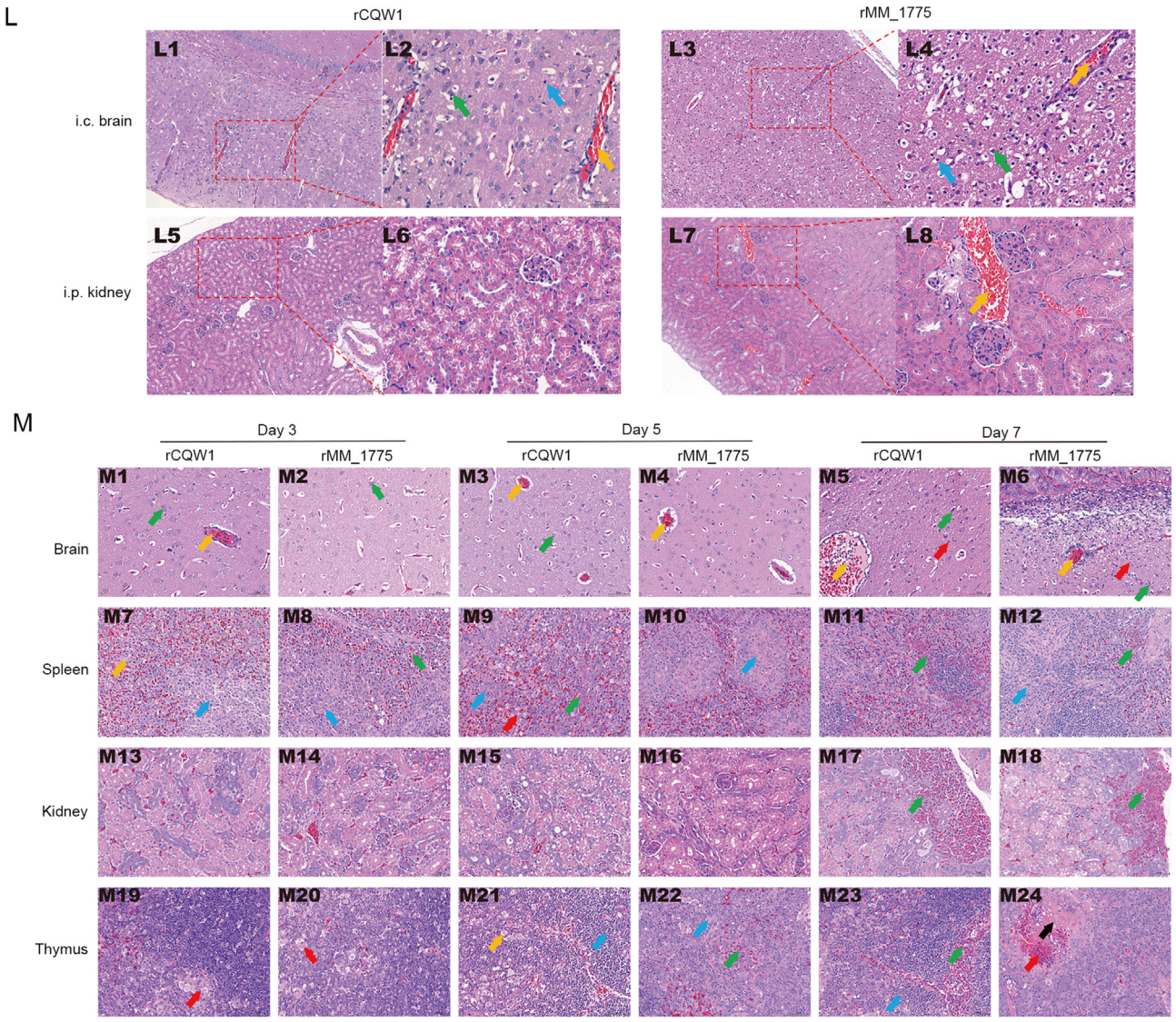

Fig. 1. (*continued*).

Fig. 1. The pathogenicity of TMUV in duckling and mice. **A** Mouse experimental design. Three-week-old Kunming female mice were infected with rMM_1775 or rCQW1 by intraperitoneal injection (i.p.) at $10^{4.5}$ $TCID^{50}$/200 μL and intracranial injection (i.c.) at $10^{4.5}$ $TCID_{50}$/50 μL. Weight changes, clinical signs and mortality were monitored for 14 days. Viremia and viral loads in the tissues were detected at 2, 5 and 8 dpi. **B** The mice infected with rCQW1 by intracranial injection displayed paralysis of two hind legs, crawling and inability to open their eyes at 6 dpi. **C** The survival curves of the Kunming mice inoculated with TMUV by the i.c. and i.p. route. **D** Body weight changes in the Kunming mice inoculated with TMUV by the i.c. and i.p. route. **E** Viral titers in the brains of the mice inoculated with rMM_1775 at 2, 5 and 8 dpi by the i.c. route were determined by BHK-21 cells. Statistical significance was determined using an unpaired *t*-test. ns, not significant; **, $P < 0.01$; ****, $P < 0.0001$. **F** SPF duckling infection experimental design. Five-day-old SPF ducklings were infected with rMM_1775 or rCQW1 by intramuscular injection at 10^5 $TCID_{50}$/200 μL. Weight changes, clinical signs and mortality were monitored for 14 days. The viremia and viral load in the tissues were detected at 3, 5 and 7 dpi. **G** Survival curves of infected ducklings. **H** Effect of TMUV on the weight gain of ducklings. The body weight of survivors in each group was measured every other day and calculated as the mean value ± SD. **I** Viral titers in the brains of ducklings inoculated with rMM_1775 or rCQW1 at 3, 5 and 7 dpi were determined by BHK-21 cells. **J** Viremia of ducklings after infection with rMM_1775 or rCQW1 at 3, 5 and 7 dpi. **K** Viral titers in the heart, liver, spleen, lung, kidney and thymus of the ducklings inoculated with rMM_1775 or rCQW1 at 3, 5 and 7 dpi were determined by BHK-21 cells. Statistical significance was determined using an unpaired *t*-test. ns, not significant; *, $P < 0.05$; **, $P < 0.01$; ***, $P < 0.001$. **L** Histopathological lesions of brain and kidney from Kunming mice infected with TMUV. Histopathological lesions from the Kunming mice infected with rCQW1 (L1, L2, L5, L6) and rMM_1775 (L3, L4, L7, L8) at 5 dpi were observed at magnifications of × 100 and × 400. Neuronal degeneration and necrosis (green arrow), vasodilation and hyperemia (yellow arrow), and microglia hyperplasia (blue arrow). **M** Histopathological lesions of tissues from ducklings infected with TMUV. Histopathological lesions of tissues from the ducklings infected with rCQW1 and rMM_1775 were observed at magnifications of × 400. (**M1**) Brain, 3 dpi, degeneration and necrosis of neurons (green arrow), vasodilation and hyperemia (yellow arrow). (**M2**) Brain, 3 dpi, degeneration and necrosis of neurons (green arrow). (**M3**) Brain, 5 dpi, degeneration and necrosis of neurons (green arrow), vasodilation and hyperemia (yellow arrow). (**M4**) Brain, 5 dpi, vasodilation and hyperemia (yellow arrow). (**M5**) and (**M6**) Brain, 7 dpi, degeneration and necrosis of neurons (green arrow), vasodilation and hyperemia (yellow arrow), microglial hyperplasia (red arrow). (**M7**) Spleen, 3 dpi, decreased number of lymphocytes in splenic nodules (blue arrow), cell necrosis (yellow arrow). (**M8**) Spleen, 3 dpi, decreased number of splenic nodules lymphocytes (blue arrow), infiltration of heterophil granulocytes (green arrow). (**M9**) Spleen, 5 dpi, decreased number of lymphocytes in splenic nodules (blue arrow), deposition of brown and yellow (red arrow), infiltration of heterophil granulocytes (green arrow). (**M10**) Spleen, 5 dpi, decreased number of lymphocytes in splenic nodules (blue arrow). (**M11**) Spleen, 7 dpi, infiltration of heterophil granulocytes (green arrow). (**M12**) Spleen, 7 dpi, infiltration of heterophil granulocytes (green arrow), increased fibroblasts (blue arrow). (**M13–M16**) Kidney, 3 dpi and 5 dpi, no obvious pathological changes were observed. (**M17–M18**) Kidney, 7 dpi, infiltration of heterophil granulocytes (green arrow). (**M19–M20**) Thymus, 3 dpi, cell swelling and vacuolation (red arrow). (**M21**) Thymus, 5 dpi, decreased number of lymphocytes (yellow arrow), cell necrosis (blue arrow). (**M22**) Thymus, 5 dpi, cell degeneration and necrosis (blue arrow), infiltration of heterophil granulocytes (green arrow). (**M23**) Thymus, 7 dpi, decreased number of lymphocytes (blue arrow), infiltration of heterophil granulocytes (green arrow). (**M24**) Thymus, 7 dpi, focal necrosis (black arrow), hemorrhage (red arrow).

injected with rCQW1 were significantly higher than those of the rMM_1775 group (Fig. 1K). At 5 dpi, viral loads in the lungs of the rCQW1 group were higher than those in the rMM_1775 group. In the kidney, the viral titer of the two experimental groups showed a very significant difference. Notably, the viruses were only detected in the serum of the rCQW1-infected ducklings, while they could not be detected in the serum of the rMM_1775-infected ducklings (Fig. 1J).

After inoculation with rMM_1775 by the i.c. route, the lesions in the brain of mice were mainly neuronal degeneration and necrosis, vasodilation and hyperemia, and microglial hyperplasia. In the brain, dilatation and hyperemia of cerebral pia and choroid plexus vessels were observed, and there were more infiltrated inflammatory cells, mainly neutrophils and lymphocytes. Vasodilatation and hyperemia, massive neuronal degeneration and necrosis, and massive gliosis were also observed in the cortical area in the mice infected with rCQW1 or rMM_1775 (Fig. 1L). However, in the hippocampal CA1, CA2 and CA3 regions, mice infected with different strains showed different lesions. In the brains of the mice infected with rCQW1, localized degeneration and necrosis of pyramidal cells, a small amount of degeneration and necrosis of pyramidal cells and a small amount of vacuolar degeneration of granulosa cells were observed in the CA1 region, CA3 region and DG region. In the rMM_1775 group, complete necrosis of pyramidal cells in the CA1, CA2 and CA3 regions of the hippocampus, complete necrosis of granulosa cells in the DG region, and massive gliosis were observed. In addition, a large amount of neuronal degeneration, necrosis and gliosis in various regions of the diencephalon were observed, as well as vasodilatation and congestion. In the kidney, no obvious gross lesions were found in the rCQW1 group (Fig. 1L5 and L6). Vasodilation and hyperemia in the renal interstitium and massive erythrocyte aggregation were observed in the mice infected with rMM_1775 by the i.p. route at 5 dpi (Fig. 1L7 and L8).

The main microscopic lesions of ducks were vasodilation and hyperemia, degeneration and necrosis of different cells and inflammatory cellular infiltration mainly consisting of heterophil granulocytes, although to varying degrees in ducks infected with different viruses. Obvious lesions were more frequently observed in the brain, spleen and thymus (Fig. 1M, Table 1). In the brain, vasodilation and hyperemia were observed mainly in the ducks infected with both rCQW1 and rMM_1775 (Fig. 1M1–M6). Degeneration and necrosis of neurons were observed in the ducks infected with rCQW1 at 3 dpi and 5 dpi (Fig. 1M1 and M3) and the ducks infected with rMM_1775 at 5 dpi (Fig. 1M4). At 7 dpi, the lesions became more severe. Degeneration and necrosis of neurons, vasodilation and hyperemia and microglia hyperplasia were observed in the ducks infected with both rCQW1 and rMM_1775, and more erythrocytes and lymphocytes were found in the lumen of the ducks infected with rCQW1 (Fig. 1M5 and M6). In the spleen, lymphoid cell depletion was a prominent feature (Fig. 1M7 and M12). At 3 dpi, degeneration and necrosis of many cells in the red pulp were observed in the ducks infected with rCQW1 (Fig. 1M7), and infiltration of heterophil granulocytes with more eosinophilic granules in the cytoplasm was observed in ducks infected with rMM_1775 (Fig. 1M8). At 5 dpi, in addition to more cell degeneration and necrosis in the red pulp, brown-yellow pigment deposition in the cytoplasm of some cells and infiltration of heterophil granulocytes could be observed in the ducks infected with rCQW1 (Fig. 1M9). At 7 dpi, infiltration of heterophil granulocytes was observed in the ducks infected with both rCQW1 and rMM_1775 (Fig. 1M11 and M12). Hyperplasia of fibrous tissue around the periarterial lymphatic sheath was also observed in the ducks infected with rMM_1775. In the kidney, at 7 dpi, infiltration of heterophil granulocytes was observed in the interstitium of the ducks infected with both rCQW1 and rMM_1775 (Fig. 1M17 and M18). No obvious pathological changes were observed at 3 and 5 dpi. In the thymus, at 3 dpi, swelling and vacuolation of small thymus cells in the medullary area were observed in the ducks infected with rCQW1 or rMM_1775 (Fig. 1M19 and M20). At 5 dpi, degeneration and necrosis of cells in the medulla area could be observed in the ducks infected with rCQW1 or rMM_1775 (Fig. 1M21 and M22). A decrease in the number of lymphocytes was observed in the ducks infected with rCQW1 (Fig. 1M21), and infiltration of heterophil granulocytes was observed in the ducks infected with rMM_1775 at 5 dpi (Fig. 1M22). At 7 dpi, a significant decrease in the area of the lobular cortex was observed in the ducks infected with both rCQW1 and rMM_1775 (Fig. 1M23 and M24). A marked decrease in the number of lymphocytes and infiltration of heterophil granulocytes in the medullary area were observed in the ducks infected with rCQW1 (Fig. 1M23), while the ducks infected with rMM_1775 showed focal necrosis and hemorrhage in the medulla (Fig. 1M24).

Table 1
The severity of microscopic lesions of ducklings infected with rCQW1 and rMM_1775 via intramuscular injection route.

Tissues	rCQW1			rMM_1775		
	3 dpi	5 dpi	7 dpi	3 dpi	5 dpi	7 dpi
Spleen	+++[a]	+++	+++	+++	+++	++
Kidney	-	-	++	-	-	++
Thymus	++	+++	+++	++	++	+++
Brain	++	++	++	+	+	++

[a] The severity of microscopic lesions: -, no lesions; +, mild; ++, moderate; +++, severe.

Duck TMUV, an emerging flavivirus that mainly infects waterfowls, has caused major losses to the duck industry since it broke out in China. Most flaviviruses are zoonotic pathogens and can invade the host's central nervous system (CNS), causing severe damage. For example, West Nile virus (WNV) infiltrates the CNS, directly infects neurons and induces neuronal cell death, and it also induces neuroinflammation (Stonedahl et al., 2020). Japanese encephalitis virus (JEV) can cause a variety of neurological symptoms, including mental status changes, focal neurologic deficits, and movement disorders (Yun and Lee, 2014). Yellow fever virus (YFV) can cause viral encephalitis in mice (Kimura et al., 2010). DTMUV, as a novel flavivirus, can also invade the CNS, causing non-suppurative encephalitis in ducklings, as well as neurological and blood-brain barrier disruption in the intermediate stages of infection (Yang et al., 2021). Here, we found that Kunming mice could be infected with mosquito TMUV by intracranial injection, with neurological symptoms of paralysis of the lower limbs, and mosquito TMUV rMM_1775 exhibited stronger pathogenicity in mice than duck TMUV rCQW1, as indicated by the weight changes and mortalities. The results were the same as those previously reported (Mao et al., 2022; Ti et al., 2016). We also confirmed that TMUV can infect SPF ducklings by intramuscular injection and can be detected in the brain, suggesting that TMUV can cross the blood-brain barrier. This finding indicated that TMUV, similar to other flaviviruses, has the ability to invade around nerves.

In this study, we found that duck TMUV rCQW1 was less pathogenic to mice. This finding was in contrast to the previous study, reporting that duck derived TMUV caused severe disease in mice by the intracerebral inoculation route (Yurayart et al., 2021). There may be two possible reasons. First, the pathogenicity of different duck TMUV strains in mice was different. We compared the sequences of a large number of ducks TMUVs and found seven amino acid differences in the E protein and NS1 between rCQW1 and other duck TMUVs which are highly pathogenic to mice. A mutation at a site on the E protein that enhances the pathogenicity of CQW1 in mice has been identified, and we are now investigating the mechanism. The second reason is the viral titer and the age of mice for inoculation. Three-week-old Kunming mice were inoculated with a lower titer ($10^{4.5}$ $TCID_{50}$) in this study. In a recent study, three-week-old Kunming mice were infected with rCQW1 with higher titers ($10^{5.25}$ $TCID_{50}$) by i.c. inoculation, and the survival rate of mice decreased significantly, only 60%. Besides, body weight started to decrease from 4 dpi compared with the control group and increased again until 8 dpi (Guo et al., 2020). While in Mao's article, 14-day-old Kunming mice were infected with rCQW1 with a low titer ($10^{4.375}$ $TCID_{50}$) by i.c. inoculation, the survival rate was 60%, and the mice developed significant clinical

symptoms, including blindness in both eyes and hind limb paralysis (Mao et al., 2022). We would select younger mice (14-day-old) or infect the mice with higher titers to investigate the pathogenicity in future.

Here, viruses were detected in most tissues, including the heart, liver, spleen, lung, kidney and thymus, in both experimental groups at 3 dpi, indicating that rCQW1 or rMM_1775 entered the body very quickly and had broad tissue tropism, which is consistent with previous reports. The pathogenicity of the virus in ducklings correlated with the virus in tissues. DTMUV was shown to invade lymphocytes and macrophages of the spleen at 2 dpi and replicate significantly from 1 dpi to 3 dpi, being eliminated from 9 dpi to 18 dpi (Sun et al., 2019). Among the investigated tissues, viral titers in spleens from experimental groups were highest at 3 dpi. Enlargement and hyperemia of the spleen could be observed at necropsy, and hematoxylin and eosin staining showed significant lymphoid cell depletion. These findings support the notion that the spleen may be a target organ and a major replication site for TMUV and several flaviviruses (Prestwood et al., 2012; Sun et al., 2019). Notably, no virus was detected in the serum of the group inoculated with mosquito TMUV rMM_1775, whereas in the group inoculated with duck TMUV rCQW1, virus could be detected at 3, 5 and 7 dpi, and the virus was gradually eliminated from the bloodstream over time. This finding is consistent with the results of Yan et al., who found that mosquito TMUV was not detectable in the blood of 12- to 15-week-old ducks through intramuscular or intranasal route at 3 dpi (Yan et al., 2018). And this may because the absence of glycosylation modification in the E protein N154 of rMM_1775, and the N153 or N154 glycosylation site is located at the “150 loop” of DI of the E protein, which could be an attachment region and influence virus transmission. As TMUV is a mosquito-borne flavivirus, this finding may also be one of the reasons that mosquito TMUV did not initially cause widespread epidemics in ducks.

Taken together, this study demonstrates that the pathogenicity of mosquito TMUV rMM_1775 strain to Kunming mice was higher. We also found that both duck TMUV rCQW1 strain and mosquito TMUV rMM_1775 strain could be detected in multiple organs of SPF ducklings, but rMM_1775 could cause systemic infection without causing obvious viremia. Therefore, this study provides experimental data for further study on the evolution and pathogenic mechanism of TMUV.

Footnotes

This work was funded by grants from the National Natural Science Foundation of China (32272976), the National Key Research and Development Program of China (2022YFD1801900), the China Central and Eastern European Countries Joint Education Project (2021092), the Sichuan Provincial Department of Science And Technology International Scientific and Technological Innovation Cooperation (2022YFH0026), the earmarked fund for China Agriculture Research System (CARS-42-17), and the Program Sichuan Veterinary Medicine and Drug Innovation Group of China Agricultural Research System (SCCXTD-2021-18). The authors declare that there are no competing financial interests regarding the publication of this paper. All animal experimental procedures were approved by the Institutional Animal Care and Use Committee of Sichuan Agriculture University in Sichuan, China (Protocol Permit Number: SYXK(川)2019-187).

All the data generated during the current study are included in the manuscript. Supplementary data to this article can be found online at https://doi.org/10.1016/j.virs.2023.07.006.

References

Chen, S., He, Y., Zhang, R., Liu, P., Yang, C., Wu, Z., Zhang, J., Wang, M., Jia, R., Zhu, D., Liu, M., Yang, Q., Wu, Y., Cheng, A., 2018. Establishment of a reverse genetics system for duck Tembusu virus to study virulence and screen antiviral genes. Antivir. Res. 157, 120–127.

Guo, J., He, Y., Wang, X., Jiang, B., Lin, X., Wang, M., Jia, R., Zhu, D., Liu, M., Zhao, X., Yang, Q., Wu, Y., Chen, S., Cheng, A., 2020. Stabilization of a full-length infectious cDNA clone for duck Tembusu virus by insertion of an intron. J. Virol Methods 283, 113922.

Kimura, T., Sasaki, M., Okumura, M., Kim, E., Sawa, H., 2010. Flavivirus encephalitis: pathological aspects of mouse and other animal models. Vet. Pathol. 47, 806–818.

Mao, L., He, Y., Wu, Z., Wang, X., Guo, J., Zhang, S., Wang, M., Jia, R., Zhu, D., Liu, M., Zhao, X., Yang, Q., Mao, S., Wu, Y., Zhang, S., Huang, J., Ou, X., Gao, Q., Sun, D., Cheng, A., Chen, S., 2022. Stem-loop I of the Tembusu virus 3'-untranslated region is responsible for viral host-specific adaptation and the pathogenicity of the virus in mice. Microbiol. Spectr. 10, e0244922.

Platt, G.S., Way, H.J., Bowen, E.T., Simpson, D.I., Hill, M.N., Kamath, S., Bendell, P.J., Heathcote, O.H., 1975. Arbovirus infections in sarawak, October 1968–February 1970 Tembusu and sindbis virus isolations from mosquitoes. Ann. Trop. Med. Parasitol. 69, 65–71.

Prestwood, T.R., May, M.M., Plummer, E.M., Morar, M.M., Yauch, L.E., Shresta, S., 2012. Trafficking and replication patterns reveal splenic macrophages as major targets of dengue virus in mice. J. Virol. 86, 12138–12147.

Stonedahl, S., Clarke, P., Tyler, K.L., 2020. The role of microglia during West Nile virus infection of the central nervous system. Vaccines (Basel) 8, 485.

Su, J., Li, S., Hu, X., Yu, X., Wang, Y., Liu, P., Lu, X., Zhang, G., Hu, X., Liu, D., Li, X., Su, W., Lu, H., Mok, N.S., Wang, P., Wang, M., Tian, K., Gao, G.F., 2011. Duck egg-drop syndrome caused by BYD virus, a new Tembusu-related flavivirus. PLoS One 6, e18106.

Sun, X., Liu, E., Iqbal, A., Wang, T., Wang, X., Haseeb, A., Ahmed, N., Yang, P., Chen, Q., 2019. The dynamic distribution of duck Tembusu virus in the spleen of infected shelducks. BMC Vet. Res. 15, 112.

Ti, J., Zhang, M., Li, Z., Li, X., Diao, Y., 2016. Duck Tembusu virus exhibits pathogenicity to kunming mice by intracerebral inoculation. Front. Microbiol. 7, 190.

Wang, X., He, Y., Guo, J., Jiang, B., Wang, M., Jia, R., Zhu, D., Liu, M., Zhao, X., Yang, Q., Wu, Y., Zhang, S., Liu, Y., Zhang, L., Yu, Y., Cheng, A., Chen, S., 2021. Construction of an infectious clone for mosquito-derived Tembusu virus prototypical strain. Virol. Sin. 36, 1678–1681.

Yan, D., Shi, Y., Wang, H., Li, G., Li, X., Wang, B., Su, X., Wang, J., Teng, Q., Yang, J., Chen, H., Liu, Q., Ma, W., Li, Z., 2018. A single mutation at position 156 in the envelope protein of Tembusu virus is responsible for virus tissue tropism and transmissibility in ducks. J. Virol. 92, e00427-18.

Yang, S., Huang, Y., Shi, Y., Bai, X., Yang, P., Chen, Q., 2021. Tembusu Virus entering the central nervous system caused nonsuppurative encephalitis without disrupting the blood-brain barrier. J. Virol. 95, e02191-20.

Yun, S.I., Lee, Y.M., 2014. Japanese encephalitis: the virus and vaccines. Hum. Vaccines Immunother. 10, 263–279.

Yurayart, N., Ninvilai, P., Chareonviriyaphap, T., Kaewamatawong, T., Thontiravong, A., Tiawsirisup, S., 2021. Pathogenesis of Thai duck Tembusu virus in BALB/c mice: Descending infection and neuroinvasive virulence. Transbound Emerg. Dis. 68, 3529–3540.

Zhu, K., Huang, J., Jia, R., Zhang, B., Wang, M., Zhu, D., Chen, S., Liu, M., Yin, Z., Cheng, A., 2015. Identification and molecular characterization of a novel duck Tembusu virus isolate from Southwest China. Arch. Virol. 160, 2781–2790.